


Fracture toughness characterization of aluminum alloy AA3003 using essential work of fracture concept

H. Mebarki¹, M. Benguediab¹  , H. Fekirini¹, B. Bouchouicha¹, F. Lebon² 

¹ Department of Engineering Mechanics, University Djillali Liabes, Sidi Bel Abbes, Algeria

² Aix-Marseille University, Mechanics and Acoustics Laboratory, France

 benguediabm@mail.com

Abstract. Lightning structures is one of the main challenges of the aviation industry today. Friction stir welding is an alternative to replace conventional assembly processes and reduce the mass of the structure. The mechanical behavior of this assembly must be determined to understand the failure mechanisms. The concept of fracture mechanics is often used to characterize the fracture of thin sheets. In this document, a global energy approach proposed to characterize the phenomenon of rupture and to determine experimentally the essential work of fracture in Aluminum Alloy welded by Friction Stir Welding process. The tests were carried out on DENT specimens welded by the process of friction stir welded and not welded specimens. The results obtained show that the not welded sheets show that the strength of the specimens welded by FSW has a low tear resistance compared to the welded specimens.

Keywords: Aluminum alloy, Fracture Toughness, DENT specimen, essential work of fracture EWF, Friction Stir Welding.

Citation: Mebarki H, Benguediab M, Fekirini H, Bouchouicha B, Lebon F. Fracture toughness characterization of aluminum alloy AA3003 using essential work of fracture concept. *Materials Physics and Mechanics*. 2023;51(3): 105-114. DOI: 10.18149/MPM.5132023_12.

Introduction

The lightness of structures is one of the main goals and challenges, aluminum alloys are widely used in many sectors such as the automobile industry, aeronautics and the military, thanks to a unique combination of properties, such as good strength to weight ratio, high corrosion resistance, easy workability and high electrical and heat conductivity [1,2]. The use of aluminum alloys assembled by Friction Stir Welding process is looked for to replace those riveted Aluminum alloys structures in many sectors such as in Aeronautics, Automobile and so on. However, the major challenge for designers is the welding of aluminum alloys [3]. Friction Stir Welding process presents many advantages over the conventional welding, such as less distortion, lower residual stresses and fewer weld defects, due to its low heat input and absence of melting and solidification process [4,5]. These important domains require the knowledge of fracture behaviour of the materials used for a sufficient safety in service.

For the ductile structures, the fracture characterization is a major challenge due to that the cracking is made in presence of an extended plasticization where the concepts of the Linear Fracture Mechanics (LFM) cannot be applied. Due to the limits of the Linear Fracture Mechanics, two parameters were introduced: namely the crack tip opening displacement (CTOD) and the J integral contour which describes well the stress distribution in the plasticized zones. One of these parameters can be used as fracture criteria. In 1961 Wells [6] had proposed the crack tip opening displacement (CTOD) as an alternative parameter to the stress intensity

factor in the case of ductile materials where important plasticization exists for a better description of the stress distribution in the plastic zones. The concept of the J -integral developed by Rice [7] in 1968 for the case of linear elastic behavior has been extended and used to solve the nonlinear elastic fracture problems for materials with elasto-plastic behavior.

The J -integral is similar to the elastic energy release rate G , but it depends on the non-elastic energy release rate according to Rice [7]. However, for a good J integral estimation the plane strain stress conditions must be satisfied according to the ASTM and ESIS recommendations [8,9].

The fracture toughness of materials is generally determined by using the concepts of elastic linear fracture mechanics. To characterize the fracture that arise at stresses below the elastic limit of the material, Linear elastic fracture mechanics are used under conditions where the plastic deformation at the tip of the crack is confined, and the breaking process is inherently fragile.

Many authors investigated the influence of FSW parameters on fracture toughness and fatigue crack growth of Aluminum alloy. For example, Moghadam et al. [10] investigated the influence of welding speed on fracture toughness and fatigue crack growth of FSW-AA2024-T351 alloy. The results showed that the tool rotational and traverse speeds affect the fracture toughness and fatigue crack growth rate, and FSW provides 18 – 49 % reductions in maximum fracture load and fracture toughness. The effect of the welding speed on Charpy impact toughness, hardness distribution and the material microstructure of the FSW-joint is also studied by Milčić et al. [11,12]. Later, the study by Milčić et al. [13,14] focuses on the fatigue behavior of Friction Stir Welding (FSW) joints. By determining the S-n curves, the highest fatigue strength was found to be at a welding speed of 116 mm/min. These authors also investigated the effect of welding speed on the quality of the butt joint by analyzing microstructure, hardness, and fracture toughness properties [15]. Ma et al. [16] studied the impact of stress ratio on the fatigue-crack growth characteristics of AA5083. The results showed that as the stress ratio increased, the rate of crack propagation also increased, other than the fracture toughness and the propagation threshold decreased.

The fracture toughness and tensile strength are two important mechanical properties of materials, and they are often interdependent. Increasing the tensile strength can result in a decrease in fracture toughness, and vice versa. In the case of friction stir welded AA7075-T651 joints, the study by Sivaraj et al. [17] showed that a solution treatment followed by water quenching and artificial aging improved the fracture toughness by 12% compared to as-welded joints. Similarly, Tao et al. [18] reported that friction welding of dissimilar titanium alloys also resulted in improved fracture toughness.

In conclusion, the results of these studies demonstrate the potential of FSW as a reliable method for joining metal components and the importance of considering the fracture toughness in the evaluation of the strength and reliability of FSW joints.

The essential work of fracture method, based on the work of Broberg [19] has been introduced by Cotterell and Reddel [20] as a method to obtain the toughness to rupture of thin ductile metal sheets. This method is based on the fact that the rupture process zone at the crack tip opening displacement is surrounded by an important plastic zone. The work made in this zone presents a dimensional and geometrical dependency which should be separated from the total work in order to obtain the essential work made in the rupture plastic zone.

The idea in separating the two regions is inspired from Broberg [19]. The first works using this approach are the works of Cotterell and Reddell [20] and de Mai and Cotterell [21] in the case of metal sheets. In many works [22-25] EWF tests were realized to characterize ductile rupture in sheets metals.

The essential work of fracture can be considered as an inverse approach of the classical fracture mechanics in characterizing the material toughness not at the initiation of the crack but

at the total separation of the specimen. The use of DENT specimen (Double Edge Notched Tension) is recommended in order to avoid buckling problems.

The principle of the technique consists of measure the load-displacement curve from tensile tests and the energy for a series of fracture samples, making sure that the ligament is fully plasticized. In this case, the total energy of fracture can be divided into two components. A component corresponds to the term (w_e) which is the essential work of fracture (EWF) dissipated in the zone of fracture process and (w_p) the non-essential work of fracture dissipated in the external plastic zone. For both metals and plastics, it has been observed that the volume of the outer region is proportional to the square of the ligament length and so in any valid set of conditions, the total energy absorbed in fracturing such a specimen, W_f , is given by the expression:

$$W_f = w_e Lt + w_p \beta L^2 t, \quad (1)$$

where β is a shape factor associated with dimensions of the plastic zone, L the ligament length between the two notches and t the sheet thickness.

Normalizing by Lt , we obtain the specific work of fracture w_f :

$$w_f = \frac{W_f}{Lt} = w_e + w_p \beta L. \quad (2)$$

Despite having several applications of aluminum alloy AA3003 in various fields such automobile, aeronautics, few researches are conducted on aluminum AA3003 welded by FSW in particular the fracture characterization. In this paper, an experimental investigation on aluminum alloy sheets welded and not welded with the special attention on the fracture characterization on DENT specimens welded by FSW process using the essential work of fracture approach.

Material

The material consists of plates of aluminum alloy of type AA3003 is a wrought aluminum-manganese family alloy with thickness $t = 2, 4$ mm. The material is supplied in the form of a sheet of dimensions $1000 \times 1000 \times 2$ mm.

The welded joint was obtained by assembling two AA3003 aluminum plates, dimensions $210 \text{ mm} \times 110 \text{ mm}$ and 2 mm thick. The friction stir welding is performed on a modified conventional machine milling. The welding direction was vertical to the rolling direction, and a 1.5° tilt was applied between the tool rotation axis and the normal direction of the sheet. The weld travel speed was 200 mm/min and the rotational speed of the FSW tool was 1400 rpm. Welding is done in a single pass to obtain the joints (Fig. 1). The parameters were chosen on the basis of work carried out by Chekalil et al. [26].



Fig. 1. Friction stir welding configuration

Tables 1 and 2 present the chemical composition and properties of base metal and welded AA3003 aluminum alloy respectively.

Table 1. Chemical composition of AA3003 [27]

Element	Al	Mn	Si	Fe	Cu	Ti	Zn
Wt. %	96.7	1.3	0.9	0.9	0.13	0.1	0.03

Table 2. Mechanical properties of base metal and welded AA3003 [17]

Material	UTS, MPa	YS, MPa	YM, MPa	% E
AA3003 Base Metal	156.9	105.7	70000	15.5
AA3003 Welded	140.1	87.1	70000	24.5

We can note that the tensile strength and yield strength of weld joints are lower than those of Base Metal, while the elongation is higher. This result is attributed to the phenomenon of recrystallization caused by the combination of thermomechanical effects related to the rotation and translation of the pion and the heat of the parts welded by FSW. This thermomechanical history causes metallurgical phenomena such as recrystallization grains and the change in precipitation state [27]. These results are confirmed for other types of aluminum [27–29]. Overall, the elastic limit and the tensile strength of the A3003 material are greatly reduced by FSW welding. The elastic limit decreases by 18.6 MPa between the base metal and the welded joint, i.e. a decrease of about 17.5 % and the tensile strength by 16.8 MPa or 10 %, these results are confirmed for other types of aluminum [28–32]. This reduction is generally due to the phenomenon of recrystallization caused by the combination of thermomechanical effects related to the rotation and translation of the pion and the heat of the parts welded by FSW [33]. On the other hand, recrystallization is accompanied by an increase in ductility, thus the strain is 0.155 for the no-welded specimens and 0.245 for the welded specimens, i.e. a difference of 0.046 corresponding to 58 % of the strain of the no-welded specimens.

Preparation of DENT specimens

The test specimens were obtained by water jet cutting of an aluminum plate of dimensions 300×150 mm and 2 mm thick for the unwelded specimens. Figure 2 represents the cutting principle and the dimensions of the DENT unwelded specimens.

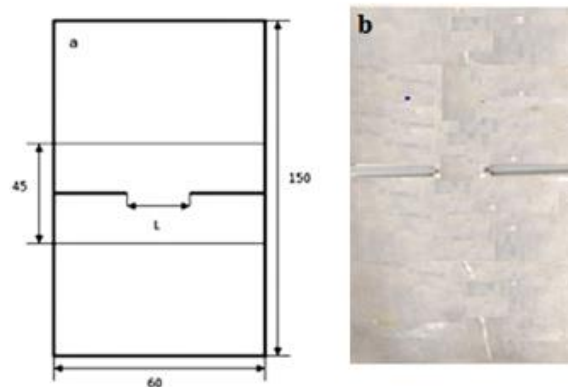


Fig. 2. (a) Geometry and dimensions of the not welded DENT specimen (dimensions are in mm). (b) Cutting by water jet of not welded specimen on plate of aluminum

The welded specimens are obtained by cutting a plate resulting from the assembly of two plates of dimensions 300×75 mm welded along the rolling direction by the friction stir welding process. Figure 3 represents the cutting principle of DENT welded specimens.

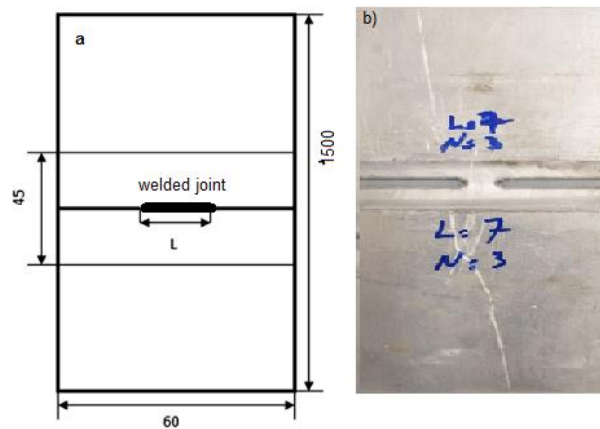


Fig. 3. (a) Geometry and dimensions of the welded DENT specimen (dimensions are in mm).
(b) Cutting by water jet of welded specimen on plate of aluminum

Determination of the essential work of fracture tests

To applying the EWF approach to evaluate the plane stress fracture toughness, the European Structural Integrity Society (ESIS)–TC 4 protocol [9] must be met. These conditions are: if L is the length of the uncracked ligament, t is the thickness and W is the width, and then the total energy absorbed during the rupture process is W_f given by relation (2).

The essential work of fracture is obtained by plotting according to the ligament L . The conditions to be verified are:

- $L > 3t$: condition of plane stresses;
- $L < W / 3$: to limit edge effects

Table 3. Number of specimens according the ESIS recommendations

Ligament Range		Number of specimens
Maximum	Minimum	
$0.33 \times W$	$0.27 \times W$	2
$0.27 \times W$	$0.20 \times W$	3
$0.20 \times W$	$0.13 \times W$	5
$0.13 \times W$	$3 \times t$	10
$0.33 \times W$	$0.27 \times W$	2

So for an uncracked ligament length L the conditions are: $W / 3 < L < 3t$. Taking into account, especially these conditions, for $W = 60$ mm, we prepared about twenty test specimens (see Table 3). The EWF tests are carried out on an INSTRON 8501 hydraulic machine with a capacity of 100 KN (Figure 4) controlled by MTS software allowing data acquisition (Load-displacement).

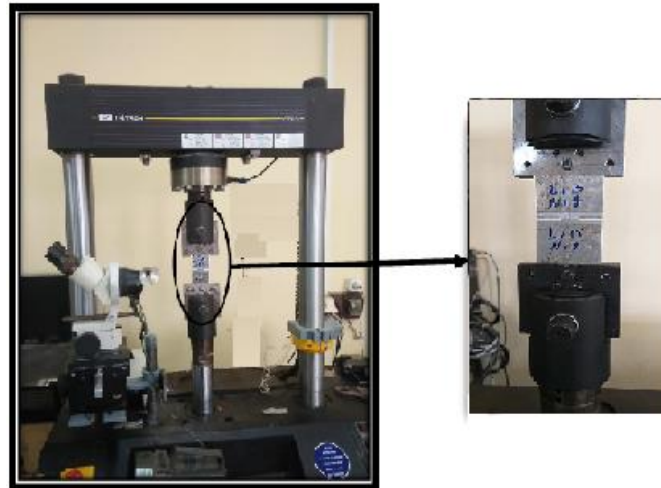


Fig. 4. INSTRON 8501 testing machine and specimen mounting

Results and discussions

The experimental results of the essential EWF fracture work obtained on the different samples with different ligaments are given in the form of force-displacement curves in Figures 5 and 6 respectively for the not welded specimens and the specimens welded by FSW. All curves follow the same shape.

The energies are calculated from the area of the curves of the load as a function of displacement. The specific energy is given by the ratio between this energy and the surface of the broken specimen, i.e. *L.t*.

It is noted that the maximum loads obtained for each ligament for the not welded specimens are greater than those obtained for the welded specimens. On the other hand, the maximum displacements of the welded specimens are much greater than those obtained for the not welded specimens. A comparison of the results is given in Table 5.

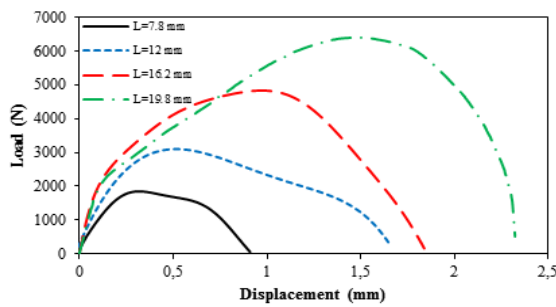


Fig. 5. Load-displacement of not welded specimen

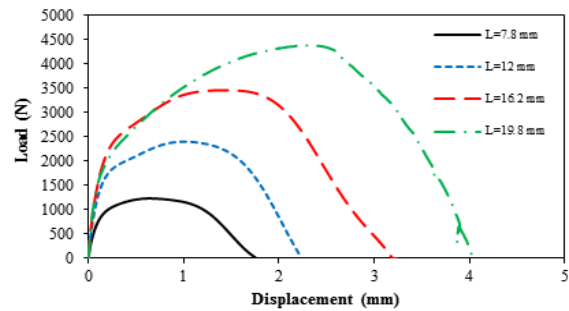


Fig. 6. Load-displacement of welded specimen

Table 4. Comparison between maximal loads and displacements for no-welded and welded specimens

Ligament Length, mm	Not welded		Welded	
	Load, N	Displacement, mm	Load, N	Displacement, mm
7.8	1844.52	0.871	1233.07	1.679
12.0	3097.88	1.635	2402.16	2.200
16.2	4833.36	1.8337	3462.33	3.154
19.8	6406.15	2.321	4385.62	4.002

Table 4 shows maximal loads and displacements for no-welded and welded specimens for each ligament, we can note that the maximum loads for not welded specimen are greater than welded specimen, on the other hand displacements for welded specimens are highest than displacements of not welded. The results obtained confirm the hypothesis that the welded joints are subjected to a phenomenon of recrystallization, as related in section "Materials".

Figure 7 presents an example of load-displacement curves for ligament length 19.8 mm (Welded specimen). The DENT specimen has been tested up to failure. The initial ligament length decreases as the load increases to reach the maximum.

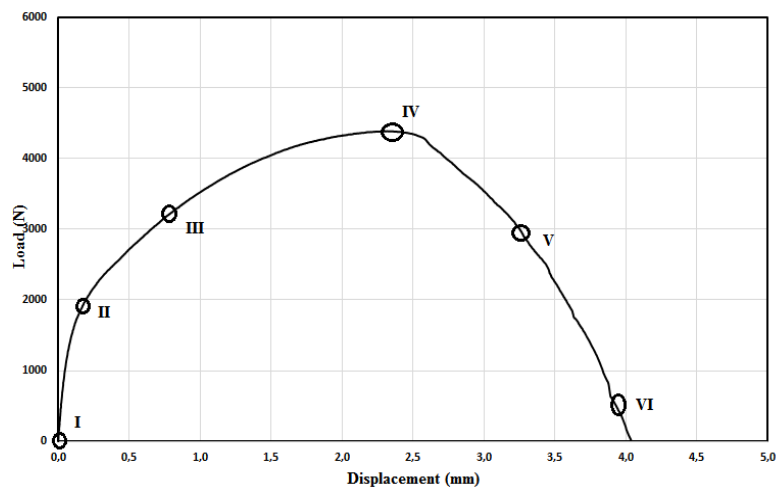


Fig. 7. Load-displacement of welded specimen

Figure 8 shows images of phases of process of deformation for welded specimens at different displacement levels identified on the load–displacement curve of Fig. 7. The observations of the specimen indicated the different phase of the deformation process during the test: I-Initial configuration; II-Crack initiation; III-Blunting; IV- Beginning of Tearing; V- Tearing and VI-Final rupture.

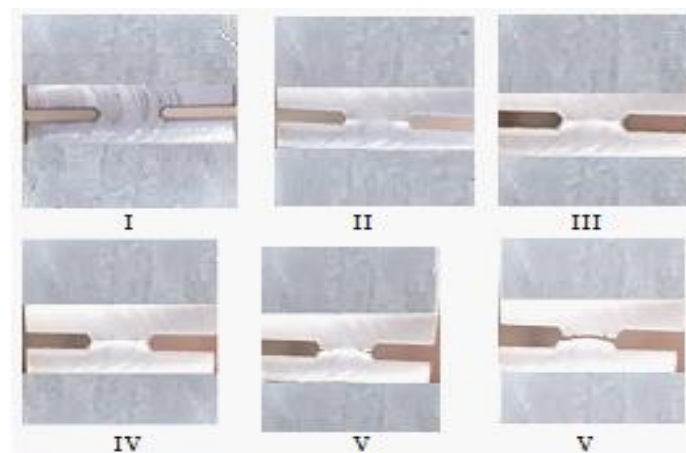


Fig. 8. Different phase of deformation process of welded specimen

The essential work of fracture as a function of the ligament of not welded specimen and of welded specimen is given by Figs. 9 and 10.

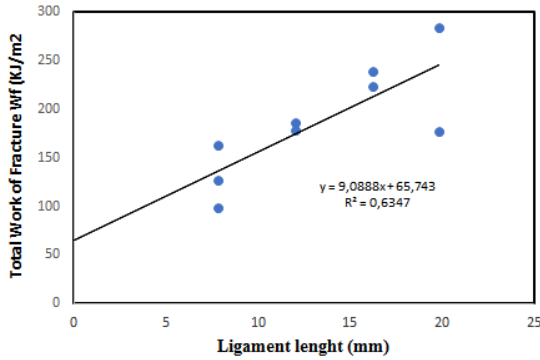


Fig. 9. Variation of total work fracture with respect to initial size of Ligament (not welded)

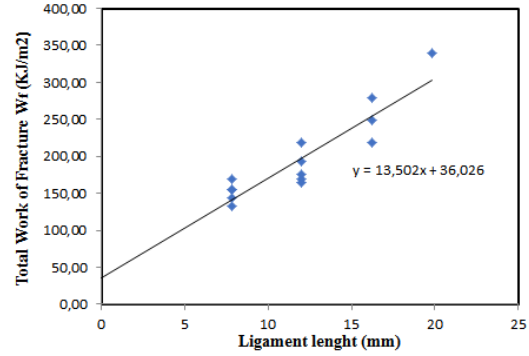


Fig. 10. Variation of total work fracture with respect to initial size of Ligament (welded)

The EWF parameters are determined by plotting the total work of rupture w_f as a function of the length of the ligament L . The value of the essential work of the rupture of w_e is obtained by extrapolation of w_f for a length of the ligament $L = 0$ and the value of $\beta.w_p$ is the slope of the line resulting from the linear regression.

The values of the essential specific work and the non-essential specific fracture work obtained for the welded specimens and the non-welded specimens are therefore grouped together in Table 5.

Table 5. EWF parameters for not welded and welded specimens

Specimen	$\beta.w_p$, KJ/m ²	w_e
Not welded	9.088	65.783
Welded	13.502	36.026

The essential work of fracture decreases by 29.75 KJ/m² between the base metal and the welded joint, i.e. a decrease of about 45.23 %. This result confirms the values of the essential specific work obtained for the tensile tests, therefore the fracture toughness of the joint welded by FSW is reduced, and this is explained by the recrystallization phenomenon observed during welding by FSW.

Conclusions

The experimental tests carried out in this work make it possible to highlight the tenacity to rupture, in terms of essential fracture work, as a suitable property of the material to estimate the ductility of the AA3003 aluminum sheets.

The EWF method allowed us to demonstrate a very ductile behavior characterized by the existence of a large phase of plastic deformation. The essential work of fracture, which is a method of characterizing the fracture of thin sheets. This method is used only on the assumption of plane stresses. In the present study, it was successfully used for the fracture characterization of FSW welded and unwelded AA3003 aluminum sheets. The results obtained show that the unwelded sheets has a better tear resistance compared to the welded sheets.

References

1. Aydin H, Demirci A. H. Wear Behavior of aged Al-Cu-Mg Alloys Sliding Against C45 Steel and SiC Abrasive Paper. *Materials Testing*. 2007;49(5): 253-257.
2. Zhou C, Yang X, Luan G. Investigation of Microstructure and Fatigue Properties of Friction Stir Welded Al-Mg Alloy. *Materials Chemistry and Physics*. 2006;98(2-3): 285-290.

3. Aydin H, Bayram A, Durgun I. The effect of postweld heat treatment on the mechanical properties of 2024-T4 friction stir-welded joints. *Materials Design*. 2010;31(5): 2568–2577.
4. Ren SR, Ma ZY, Chen LQ. Effect of welding parameters on tensile properties and fracture behavior of friction stir welded Al-Mg-Si Alloy. *Scripta Materiala*. 2007;56(1): 69-72.
5. Zhao YH, Lin SB, Wu L, Qu FX. The influence of pin geometry on bonding and mechanical properties in friction stir welds Al alloys. *Materials Letters*. 2005;59(23): 2948–2952.
6. Wells AA. Unstable Crack Propagation in Metals. In: *Cleavage and Fast Fracture. Proceedings of the Crack Propagation Symposium*. Cranfield, UK; 1961. p.84.
7. Rice JE. A path independent integral and the approximate analysis of strain Concentrations by notches and cracks. *Journal of Applied Mechanics*. 1968;35(2): 379-386.
8. ASTM E 813-89: Standard test method for J_c a measure of fracture toughness. *Annual Book of ASTM Standards*. Vol. 03.01, 1989.
9. ESIS. ESIS procedure for determining the fracture behavior of materials. *Ed. GKSS-Forschungszentrum Geesthacht: Karl-Heinz Schwalbe*. 1992: 2-9.
10. Moghadam DG, Farhangdoost K. Influence of welding parameters on fracture toughness and fatigue crack growth rate in friction stir welded nugget of 2024-T351 aluminum alloy joints. *Trans. Nonferr. Met. Soc. China*. 2016;26: 2567–2585.
11. Milčić M, Vuherer T, Radisavljević I, Milčić D, Kramberger J. The influence of process parameters on the mechanical properties of friction-stir-welded joints of 2024 T351 aluminum alloys. *Mater. Technol*. 2019;53: 771–776.
12. Milčić M, Vuherer T, Radisavljević I, Milčić D, Kramberger J, Andjelković B. Mechanical behaviour of Al 2024 alloy welded by friction stir welding. *IOP Conf. Series: Mater. Sci. Eng*. 2018;393: 1–9.
13. Vuherer T, Kramberger J, Milčić D, Milčić M, Glodež S. Fatigue behaviour of friction stir welded AA-2024 aluminium alloy sheets. *IOP Conf. Series: Mater. Sci. Eng*. 2019;659: 1–8.
14. Milčić M, Burzić Z, Radisavljević I, Vuherer T, Milčić D, Grabulov V. Experimental investigation of fatigue properties of FSW in AA-2024-T351. *Procedia Struct. Integr*. 2018;13: 1977–1984.
15. Milčić M, Milčić D, Vuherer T, Radović L, Radisavljević I, Đurić A. Influence of Welding Speed on Fracture Toughness of Friction Stir Welded AA2024-T351 Joints. *Materials*. 2021;14: 1561.
16. Ma M, Wang B, Liu H, Yi D, Shen F, Zhai T. Investigation of fatigue crack propagation behavior of 5083 aluminum alloy under various stress ratios: Role of grain boundary and Schmid factor. *Mater. Sci. Eng. A*. 2020;773: 138871.
17. Sivaraj P, Kanagarajan D, Balasubramanian V. Effect of post weld heat treatment on fracture toughness properties of friction stir welded aa7075-t651 aluminium alloy joints. *Journal of Manufacturing Engineering*. 2014;9(2): 110-115.
18. Tao BH, Li Q, Zhang YH, Zhang TC, Liu Y. Effects of post-weld heat treatment on fracture toughness of linear friction welded joint for dissimilar titanium alloys. *Materials Science and Engineering: A*. 2015;634: 141-146.
19. Broberg KB. Critical review of some theories in fracture mechanics. *International Journal of Fracture*. 1968;4(1): 11-18.
20. Cotterell B, Reddel JK. The essential work of plane stress ductile fracture. *International Journal of Fracture*. 1977;13(3): 267–277.
21. Mai YW, Cottrell B. On the essential work of ductile fracture in polymers. *International Journal of Fracture*. 1986;32(2): 105–125.
22. Wang HW, Kang YL, Zhang ZF, Qin QH. Size effect on the fracture toughness of metallic foil. *International Journal of Fracture*. 2003;123: 177-185.

23. Aberkane M, Ould-Ouali M. Fracture characterization of ST37-2 thin metal sheet with experimental and numerical methods. *Key Eng. Mater.* 2011;473: 396–403.
24. Bensaada R, Elmansba M, Ferhoum R, Sidhoum Z. Ductile Fracture Study of Stainless Steel AISI 304L Thin Sheets Using the EWF Method and Cohesive Zone Modeling. *Journal of Failure Analysis and Prevention.* 2017;18: 1181–1190.
25. Pardoën T, Hachez F, Marchioni B, Blyth PH, Atkins AG. Mode I fracture of sheet metal. *Journal of the Mechanics and Physics of Solids.* 2004;52(2): 423-452.
26. Chekalil I, Miloudi A, Planche MP, Ghazi A. Prediction of mechanical behavior of friction stir welded joints of AA3003 aluminum alloy. *Frattura ed Integrità Strutturale.* 2020;54: 153-168.
27. Tan YB, Wang XM, Ma M, Zhang JX, Liu WC, Fu RD, Xiang S. A study on microstructure and mechanical properties of AA3003 Aluminum Alloy Joints by underwater friction stir welding. *Materials Characterization.* 2017;127(1): 41-52.
28. Balasubramanian V. Relationship between base metal properties and friction stir welding process parameters. *Materials Science and Engineering: A.* 2008;480(1-2): 397-403.
29. Cavaliera P, Squillace A. High temperature deformation of friction stir processed 7075 aluminum alloy. *Materials Characterization.* 2005;55(2): 136-142.
30. Truant X. *Study and Modeling of the mechanical behaviour of structural panels welded by friction stir welding (FSW).* PhD Thesis. Paris, France: PSL Research University; 2018.
31. Elangovan K, Balasubramanian V. Influence of pin profile and rotational speed of the tool on the formation of friction stir processing zone in AA2219 aluminium alloy. *Materials Science and Engineering: A.* 2007;459(1-2): 718.
32. Mishra RS, Ma ZY, Mahoney MW. Superplastic deformation behaviour of friction stir processed 7075al alloy. *Acta Materialia.* 2002;50(17): 4419-4430.
33. Genevois C. *Genèse des microstructures lors du soudage par friction malaxage d'alliages d'aluminium de la série 2000 et 5000 et comportement mécanique résultant.* PhD Thesis. National France: Polytechnic Institute of Grenoble; 2004. (In-French)

THE AUTHORS

H. Mebarki

e-mail: 1993hicham76@gmail.com

M. Benguediab 

e-mail: benguediabm@gmail.com

H. Fekirini

e-mail: Fekirini.hamida@gmail.com

B. Bouchouicha

e-mail: benattou_b@yahoo.fr

F. Lebon 

e-mail: lebon@lma.cnrs-mrs.fr